An Investigation of the Mechanism of Liquid Injection into Fluidized Beds

Stefan Bruhns and Joachim Werther
Chemical Engineering I, Technical University Hamburg–Harburg, D-21071 Hamburg, Germany

DOI 10.1002/aic.10336
Published online in Wiley InterScience (www.interscience.wiley.com).

The mechanism of liquid injection into fluidized bed reactors was investigated by injecting water and ethanol, respectively, into a pilot-scale bubbling fluidized bed (cross section: 1 × 0.5 m) that was kept at temperatures between 120 and 180°C. Quartz sand and FCC catalyst were used as bed materials. The injected liquid was found to form agglomerates with the bed particles at the nozzle exit and become transported into the bed interior by mixing of the large-scale solids. There the liquids evaporate from the surface of the particles. © 2005 American Institute of Chemical Engineers *AIChE J,* 51: 766–775, 2005

Introduction

Fluidized bed reactors are widely applied in chemical engineering. Their applications range from physical operations, like agglomeration and coating of particles, to chemical reactors for the heterogeneous gas-phase catalysis.[1] With respect to the latter application, some industrial-scale reactor concepts use the liquid injection of reactants, such as the fluid catalytic cracking (FCC) process,[2] the aniline synthesis by BASF,[3] and the production of polyethylene in the super-condensed mode.[4] The liquids are injected into the reactor, evaporate in the interior of the fluidized bed, and the generated gases undergo the respective catalytic reactions.

The liquid injection of reactants provides many advantages compared to the injection of reactants in the gaseous form. Because the liquid reactants evaporate in the interior of the fluidized bed, this technology allows cost savings for the evaporation in external heat exchangers. It also minimizes the risk of hot-spot formation near the reactant feed point by providing an efficient cooling by the latent heat of evaporation, especially in the case of strongly exothermic reactions. A detailed knowledge of the mechanism of liquid injection into fluidized bed reactors is required, not only for the engineering design but also for the safe and economic operation on the industrial scale.

In the early stages of modeling the liquid injection into fluidized bed reactors, it was often assumed that the injected liquid evaporates instantaneously at the nozzle exit.[5] The characteristics of the subsequent penetration were assumed to be the same as those of gas jets. Another approach found in the literature is the assumption of feed droplets, which are instantaneously generated by atomization at the nozzle exit. These droplets were modeled to move and evaporate individually within the gas phase of the dense gas–solid flow of the fluidized bed.[6–8] In the case of fluidized bed granulation, the instantaneous generation of droplets is also assumed but these droplets are then assumed to hit the fluidized bed solids and to form a liquid layer on the particles' surface, which evaporates from there.[9,10]

Several experimental investigations have dealt with the injection of liquids into fluidized beds. With respect to fluidized bed granulation, Smith and Nienow[11] detected, with the aid of X-ray imaging, a spraying zone that extended 5 cm from the nozzle exit into the bed. They also measured differences between the mean bed temperature and the local temperature in this zone. Based on this, Maronga and Wnukowski[12] measured not only local temperature changes but also changes in the air humidity that were caused by the liquid injection. They identified three zones: (1) a *spraying zone* near the nozzle, where droplets were generated and particles were wetted by these droplets; (2) a *drying zone*, where liquids evaporated from the surface of wetted particles; and (3) a *heat-transfer zone*, where particles were heated up. Similar results were obtained by other research groups.[13]

Different from fluidized-bed granulation, where the mean temperature is near or below the boiling point of the injected

S. Bruhns is currently at BASF AG, GCT/T-L540, D-67056 Ludwigshafen, Germany.
Correspondence concerning this article should be addressed to J. Werther at werther@tu-harburg.de.

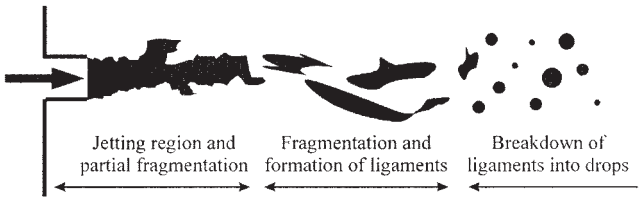

Figure 1. Atomization of liquids in gaseous environments.

Adapted from Lefebvre.[18]

liquid, fluidized-bed reactors are usually operated at higher temperatures. In the FCC process, the liquid feedstock with a boiling point of 200–300°C is injected into the riser, which is operated at 600–700°C. Therefore, Gu et al.[14] used rapidly evaporating nitrogen as a test liquid, and confirmed the existence of an evaporation zone within the riser but disproved the assumption of instantaneous evaporation at the nozzle exit. This finding was later verified by sophisticated X-ray measurements by Skouby[15] and Newton et al.[16] Another example is the fluidized bed coking process, where Knapper et al.[17] investigated the coating of atomized bitumen feed onto solid coke particles, using a sophisticated tracer technique, and found that wetted agglomerates were formed in the immediate vicinity of the feed nozzle.

Even without the interaction of the injected liquid and the gas–solid flow in the fluidized beds, the atomization of liquids in a gaseous environment is already a complex process (cf. Figure 1). The simplest idea is that the liquid flows out of an orifice and forms a liquid jet. Within a few centimeters from the nozzle exit, the liquid jet becomes fragmented by internal turbulence and by the shear with the surrounding gas. Ligaments are generated in fragmentation, which may further break down into drops.[18] Once droplets are formed, they provide a huge surface area for heat and mass transfer, which results in fast evaporation. However, high mass fluxes of liquids need to be processed in technical applications using so-called dense sprays. For dense sprays, the characteristics of evaporation differ substantially from the evaporation of idealized single droplets, which is attributed not only to the hindered formation of droplets by interactions with one another but also to transport limitations in heat and vapor transfer between the dense spray core and the gaseous environment.[19]

Therefore Zhu et al.[20] investigated both—the evaporation of a liquid nitrogen jet in co-current gas flow only and the transition toward gas–solid flow with a solid volume concentration up to 1.5%. The extent of the evaporation zone was observed by CCD camera recordings and temperature measurements. When injecting liquid nitrogen at a flow rate of 0.5 g/s into a gas flow at 2.1 m/s, they measured an evaporation zone up to a distance of 12 cm from the injector. The evaporation zone was marked by temperatures near the boiling point. The authors measured a decrease in the penetration length from 12 cm, with no solids present, to 7 cm, within a very dilute gas–solid flow of 1.5% solids volume concentration. However, these conditions differ significantly from the situation at the injection level of FCC riser-type reactors with solid volume concentrations of 20–30%.

After a review of the published experimental techniques, it seems that a single measurement technique alone cannot elucidate the complex processes within the three-phase flow structure. In particular, laboratory-scale equipment limits the extent of the flow structure and the portability to industrial-scale applications. Therefore, in the present work an experimental investigation on the mechanisms of liquid injection into fluidized bed reactors has been performed on the pilot scale. The individual processes have been monitored not only by measuring the local temperatures and the local concentrations of vaporized feed but also by measuring local solids concentrations and detecting liquids with the aid of capacitance probes.

The scope of the present work was focused on answering the following questions:

(1) How does the liquid feed penetrate the fluidized bed—like a spray or like a liquid column?

(2) How does the liquid feed distribute inside the fluidized bed—by individually moving liquid droplets or by wetted particles?

(3) How strongly is the flow structure of the fluidized bed affected by the liquid injection and what is the influence of the operating conditions?

Experimental Setup

An overall sketch of the experimental unit is shown in Figure 2. The key element of the experimental unit is the fluidized bed. The fluidizing air was supplied by a roots blower, with a maximum volumetric flow of 2500 m^3/h. An electrical air heater was used to heat the fluidizing air at a power of 40 kW. To provide more heat for the evaporation of injected liquids, a bundle of electrical heating rods, having a power of 70 kW, was immersed in the fluidized bed. A thermocouple located within the fluidized bed was used for temperature control of the bed. The bed temperature was limited to 200°C because of the thermal stability of the sealing material. The apparatus was thermally insulated to minimize heat losses and to prevent the condensation of liquids at the wall. The fluidizing air was cleaned in an internal cyclone and was subsequently cooled in a water-cooled condenser, where the injected liquid was condensed for disposal. The resulting saturated gas flow was mixed with ambient air to avoid condensation in the fabric filter. Finally, the gas was passed through an induction fan and vented to the atmosphere.

A more detailed sketch of the fluidized bed apparatus is shown in Figure 3. The total height of the apparatus was approximately 5 m. The fluidized-bed section had a cross-

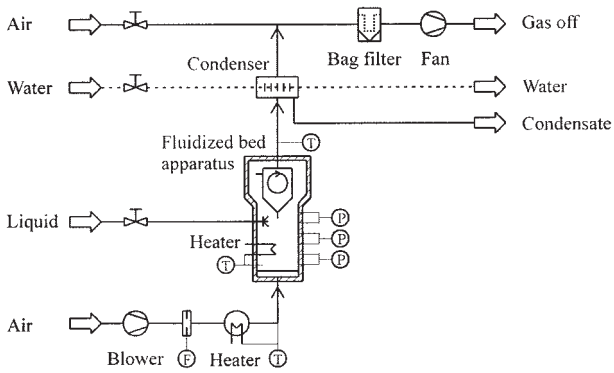

Figure 2. Experimental setup.

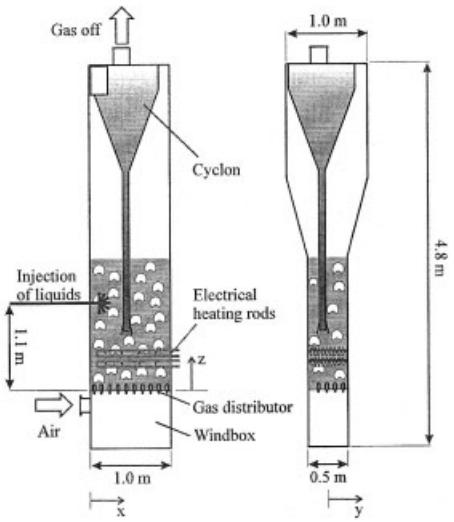

Figure 3. Fluidized-bed apparatus.

sectional area of 1 × 0.5 m and the freeboard had a cross-sectional area of 1 × 1 m. The expansion of the cross section was necessary to reduce the entrainment of fluidized particles and to provide sufficient space for the internal cyclone without accelerating the gas–solid flow in this section. The cyclone, having a diameter of 0.85 m, was fixed at the top of the apparatus. The dipleg of the cyclone was immersed into the fluidized bed for the direct return of separated particles. The gas distributor was equipped with 40 bubble caps. The tube bank of 28 U-shaped heating rods was mounted at levels between 0.2 and 0.5 m above the gas distributor. The heating rods were 9 mm in diameter. The spacing between the heating rods was chosen to be very wide, at approximately 5 cm, to minimize the disturbance of the overall gas–solid flow in the fluidized bed. The injector nozzle was mounted in the center of the front plate at a height of 1.1 m above the gas distributor.

During the experiments the fluidized-bed apparatus was filled with solids to a fixed bed height of 1.8 m. Two types of bed solids were used in the present experimental investigation: spent FCC catalyst (Sauter mean particle diameter $d_p = 70$ μm; minimum fluidization velocity $u_{mf} = 0.2$ cm/s in air at ambient conditions) and quartz sand ($d_p = 120$ μm; $u_{mf} = 3$ cm/s). The spent FCC catalyst was provided by Deutsche Shell AG (Hamburg, Germany). The fluidized-bed unit was operated in all experiments at a constant superficial gas velocity of 0.3 m/s, which is well above the minimum fluidization velocity of both bed materials.

Industrial applications of liquid injection into fluidized reactors primarily process organic liquids, which are difficult to handle. These liquids are either toxic or inflammable and in most cases even both. Two test liquids—water and ethanol—were used because of easy handling. The majority of experiments were performed with water. However, among the properties of water is its extremely high heat of evaporation of 2500 kJ/kg, which differs significantly from heats of evaporation of organic liquids in technical applications. The heat of evaporation of crude oil in the FCC process, for instance, is approximately 460 kJ/kg. Thus, additional experiments were performed with ethanol, which has a lower heat of evaporation, at 730 kJ/kg.

Different types of injection nozzles were tested. Characteristics of the investigated nozzles are listed in Table 1. Two-fluid nozzles were applied with a fan-spray pattern and full-cone spray pattern, respectively. Besides the two-fluid nozzles, single-fluid fan-spray nozzles of different spraying angles were also tested. The slot widths of the single-fluid nozzles were 0.25 and 0.8 mm, respectively. Single- and two-fluid nozzles differed in the size of the droplet generated for the given operating conditions. In case of the single-fluid nozzle with 60° fan-spray pattern, a mean droplet size of 300–400 μm was measured by the supplier for the atomization of 40–100 L/h water in a gaseous environment at ambient conditions. Under similar conditions, the air-assisted two-fluid fan nozzle (no. 4 in Table 1) by Lechler yielded a mean droplet size of 40–90 μm. Two different types of two-fluid nozzles were used in the present experimental investigation: internally and externally mixed nozzles. Internally mixed two-fluid nozzles are operated such that the liquid and the atomizing gas are premixed inside the nozzle. In the case of externally mixed nozzles, the liquid and the atomizing gas come into contact directly at the nozzle exit. The design of the nozzles used is shown in Figure 4.

A number of different measurement techniques were applied in the present experimental investigation. Fast-response thermocouples of 0.25 mm diameter were used for the measurement of local temperatures near the injection nozzle. These thermocouples register an instantaneous rise in temperature from 20 to 100°C, with a response time of 63 ms. Gas suction probes were applied for the measurement of local gas concentrations: that is, the concentration of vaporized test liquids (water and ethanol) and the concentration of tracer gas (carbon dioxide), which was added to the atomizing gas of two-fluid nozzles.

The overall arrangement of the measurement system for gas analysis is schematically shown in Figure 5. Gas was sucked off locally in the fluidized bed apparatus by a gas-suction probe. The suction probe had an outer diameter of 10 mm and filter tip of sintered bronze prevented the penetration of particles into the gas analyzer. The temperature level within the tubes, the pump, and the gas analyzer was controlled at 150°C to avoid condensation. The concentration of vaporized water or ethanol was determined from the partial pressure of oxygen in the gas sample (Oxygen Analyzer 3001M, Fisher-Rosemount, Orrville, OH). For the gas analysis of carbon dioxide, a condenser was arranged in front of the carbon dioxide gas analyzer

Table 1. Details of the Nozzles Used

Nozzle	Basic Design	Supplier	Model No.
1	Single-fluid fan spray 60°	BETE Fog Nozzle, Inc., Greenfield, MA	1/8NF03606
2	Single-fluid fan spray 120°	BETE Fog Nozzle, Inc., Greenfield, MA	1/8NF031206
3	Two-fluid externally mixed full cone spray 20°	Lechler GmbH, Metzingen, Germany	156.326.16.11
4	Two-fluid internally mixed fan spray 60°	Lechler GmbH, Metzingen, Germany	156.442.16.11

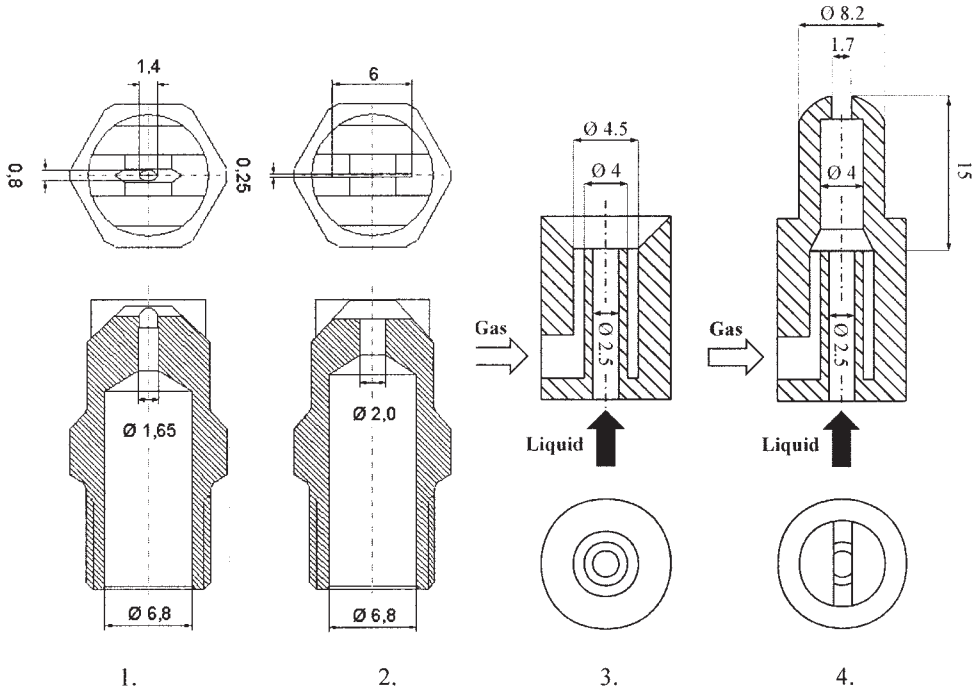

Figure 4. Design of the nozzles used.

Single-fluid fan nozzle of a spraying angle of 60° (1) and 120° (2); externally mixed two-fluid full-cone nozzle with spraying angle of 20° (3); internally mixed two-fluid fan nozzle with spraying angle of 60° (4) (the dimensions of the annular gap are the same as for the externally mixed nozzle).

(BINOS, Leybold-Heraeus GmbH, Hürth, Germany). There, the vapor content of the injected test liquid was removed by the condenser to analyze the gas concentration on a dry basis.

The capacitance measurement system for the present experimental investigation was previously used by Wiesendorf and Werther.[21] Basically, it consists of a needle capacitance probe (10 mm in diameter), a capacitance measuring instrument, and a data-acquisition system. The two-channel capacitance probes can be used for the measurement of local solids volume concentrations as well as the measurement of solids velocities by the cross-correlation technique. Because the dielectric constant of liquid water is extremely high, the capacitance probes can also be used for the local detection of liquid water within the dense gas–solid flow of fluidized beds.

Results and Discussion

In a first series of experiments, the fluidized-bed apparatus was operated with spent FCC catalyst as fluidized bed solids.

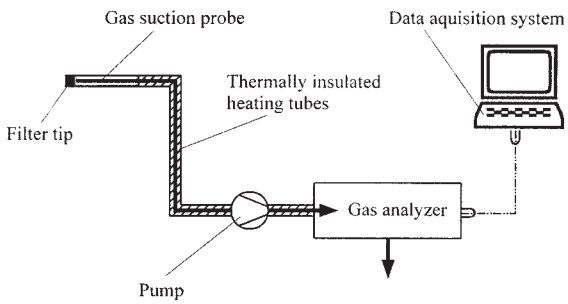

Figure 5. Measurement system for gas analysis.

The superficial gas velocity was 0.3 m/s and the bed temperature was kept constant at 153°C. Water was injected at a flow rate of 50 L/h with a single-fluid nozzle of fan-spray pattern and a spraying angle of 60°. The nozzle was located at the center of the front wall ($x = 0$ cm, $y = 0$ cm) at a height of $z = 110$ cm above the gas distributor. The temperature was measured with a fast-response thermocouple. The local mean temperatures were determined by averaging over a sufficient period of 5–10 min. It should be noted that the measured mean temperature is influenced by the volume-specific heats of injected liquid, dry/wetted solid particles, fluidizing gas and vapor, and the latent heat of evaporating liquid. The temperature measurements herein are taken as one indicator among others of the mechanisms governing the injection of a liquid into a dense bubbling fluidized bed. A more in-depth interpretation of the temperature measurements is possible on the basis of a model that includes liquid spreading and evaporation as well as the interaction between the spray jet and the fluidized bed. Such a model has also been developed within the framework of the dissertation of one of the present authors[23] and has been published elsewhere.[24]

The results are shown in Figure 6, where a dashed line marks the nozzle's ideal spraying angle of 60°. The local mean temperature in the fluidized bed rapidly rises from the inlet temperature of 20 to 60°C within the first few millimeters from the nozzle exit. With increasing distance, the mean temperature steeply rises to the boiling point at 100°C and reaches the fluidized bed temperature of 153°C at a distance of 10 cm from the nozzle exit.

Two interesting phenomena can be observed from the measured distribution of mean temperatures in the fluidized bed.

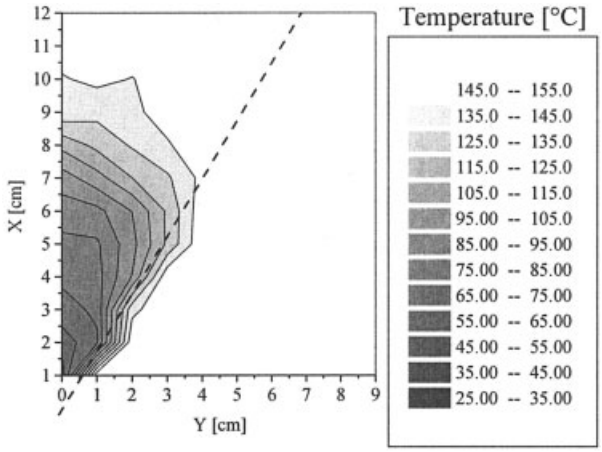

Figure 6. Mean temperatures near the nozzle at $z = 110$ cm.

Single-fluid fan nozzle no. 1, spray angle 60°; 50 L/h water. Liquid momentum flux 0.206 N; FCC bed at 153°C.

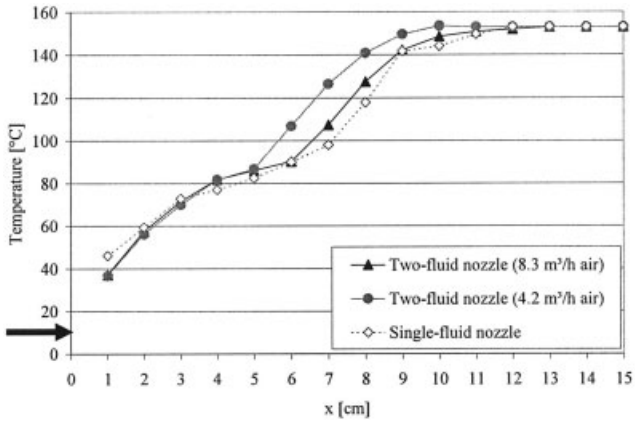

Figure 8. Mean temperatures along the distance x from the nozzle at $z = 110$ cm and $y = 0$ cm.

Single-fluid fan nozzle no. 1 and two-fluid fan nozzle no. 4, spraying angle 60°; 50 L/h water; FCC bed at 153°C. The liquid momentum fluxes of the two nozzles are 0.206 and 0.125 N, respectively; the black arrow denotes here and in the following figures the inlet temperature of the injected liquid.

First, the region where temperature deviations are caused by the liquid injection is only 10 cm in depth. Second, the spatial pattern of this change in local temperature corresponds remarkably well to the nozzle's ideal spraying angle of 60°. It seems that the small extent of the injection zone is attributable to the well-known temperature homogeneity of fluidized beds, which is caused by the intense gas–solid mixing. However, the conservation of the spray pattern is rather remarkable under the conditions of vigorous gas–solids motion in the fluidized bed.

Another experiment was performed under the same operating conditions but with a fan-type single-fluid nozzle of a different spraying angle, that is, 120°. The measured distribution of local time-averaged temperatures in the fluidized bed is shown in Figure 7. A wider spraying angle of the nozzle obviously leads to a wider distribution of the liquid feed. As a consequence, the penetration depth became further reduced to a distance of 8 cm from the nozzle exit, where a temperature difference was detectable between the mean bed temperature of 153°C and the measured temperature. As indicated by the dashed line in the chart, the spraying angle of 120° is also conserved in the measured temperature distribution. This conservation of the spray pattern under fluidized-bed conditions was also observed for other types of nozzles, such as single- and two-fluid nozzles with cone and fan-spray pattern, respectively.

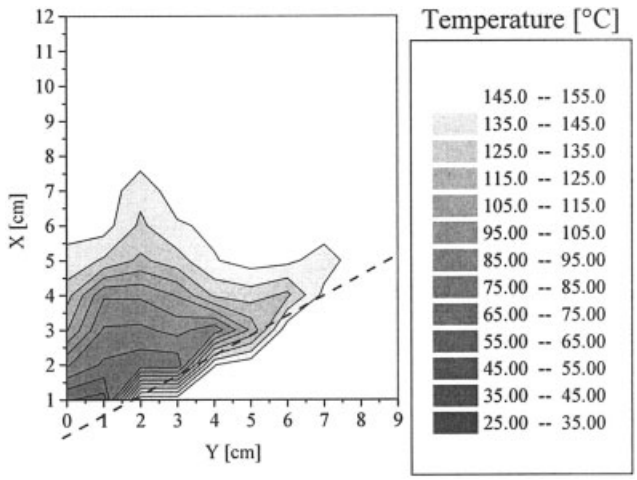

Figure 7. Mean temperatures near the nozzle at $z = 110$ cm.

Single-fluid fan nozzle no. 2, spray angle 120°; 50 L/h water. Liquid momentum flux 0.206 N; FCC bed at 153°C.

The spray pattern shown in Figures 6 and 7 is in a characteristic way different from what is known for sprays in a pure gas environment. For the atomization in a gaseous environment, the radial distribution of the liquid flux is strongly influenced by the entrainment of gas from the surrounding. The entrainment of gas results in a transport of fine droplets into the core of the spray and, consequently, a low flux at the "edge." As shown in the present experiments, the situation in a fluidized bed is different where the process is dominated by the presence of a dense gas–solid flow. Because the formation of fine droplets is hindered, which in a pure gas environment would migrate into the core, the flux is more pronounced at the edges under fluidized bed conditions.

Despite the fact that the spray patterns of different nozzles can be identified from the measured temperature distribution, there should be some difference in penetration depth for the injection with single-fluid nozzles and with two-fluid nozzles, given the differences in the generated droplet size distribution. A comparison was thus made between temperature profiles measured for the liquid injection with single-fluid and two-fluid nozzles (cf. Figure 8). The test liquid water was injected at a flow rate of 50 L/h using both types of nozzles with a fan-spray pattern and an opening angle of 60°. The internally mixed two-fluid nozzle was supplied with atomizing air of 8.3 and 4.2 m^3/h, respectively. These air volume flows are equivalent to momentum fluxes of 1.93 and 0.96 N, respectively, where the momentum flux was calculated as the product of air exit velocity and air mass flow.

For the presently used flow rate of 50 L/h water the single-fluid nozzle generates droplets with a mean diameter of 400

μm in a gaseous environment at ambient conditions, according to the supplier's information. Under the same operating conditions, the two-fluid nozzle generates in a pure gas environment 90-μm droplets for the supply of 4.2 m^3/h of atomizing air and 50-μm droplets for an atomizing air flux of 8.3 m^3/h. The momentum fluxes of the air in the latter case are 1.93 and 0.96 N, respectively. In the case of the single-fluid nozzle, the liquid momentum fluxes are based on the equivalent diameter of the narrowest cross-section. The resulting liquid momentum flux is 0.206 N for the single-fluid nozzle and 0.125 N for the two-fluid nozzle. We see from Figure 8 that neither the additional help of the atomizing air in the case of the two-fluid nozzle, compared to the single-fluid nozzle, nor the increase of atomizing air flow leads to a substantial effect with respect to the penetration of the jet. On the contrary, the measured temperature profiles are almost identical for the two types of nozzles. We observe that only the higher flow rate of the atomizing air causes a slightly deeper penetration.

After all, the performance of different nozzles for the liquid injection into fluidized beds is almost independent of the characteristic droplet distribution measured in a gaseous environment. It rather seems that no atomization occurs under fluidized bed conditions and the momentum of the liquid feed is the only factor that promotes the penetration into the fluidized bed. However, a more detailed analysis on the performance of internally and externally mixed two-fluid nozzles revealed further interesting insights into the mechanism of liquid injection into fluidized beds.

The difference between externally mixed and internally mixed two-fluid nozzles is in the process of atomization. For externally mixed nozzles, the liquid feed comes into contact with the atomizing gas at the nozzle exit only. For internally mixed nozzles, the liquid feed and the atomizing gas are already mixed in the interior of the nozzle. Therefore, internally mixed two-fluid nozzles are expected to preatomize the liquid feed within the nozzle.[18]

For these experiments the fluidized bed was operated at the same conditions as discussed above. For both types of two-fluid nozzles, the flow rate of atomizing gas was kept constant at 8.3 m^3/h. Because the geometry of the annulus for the gas flow inside the nozzle is the same for both nozzles used here the exit velocities are the same. Moreover, although the air momentum fluxes with 1.93 N, the flow rate of the injected liquid was increased from 0 to 25, 50, and 75 L/h in the respective experiments. The temperature profiles were measured and the results are shown in Figures 9 and 10. It was observed for the internally mixed nozzle that the higher the flow rate of the injected liquid, the higher the penetration depth in the measured temperature profile. The maximum extent of the temperature profile was 8 cm for the injection of 25 L/h of the test liquid water. An increase in the feed rate of the injected liquid to 75 L/h leads to a maximum extent of the temperature profile of 14 cm.

Different results were obtained for the experiments with the aid of an externally mixed two-fluid nozzle. There, a flow rate of 25 L/h of the injected liquid caused a maximum extent of the temperature profile of 13 cm. This is a higher penetration depth compared to that of the internally mixed two-fluid nozzle. However, an increase in the flow rate from 25 to 75 L/h leads to an unexpected reduction in the maximum penetration depth of 9 cm. For externally mixed nozzles, it seems that the

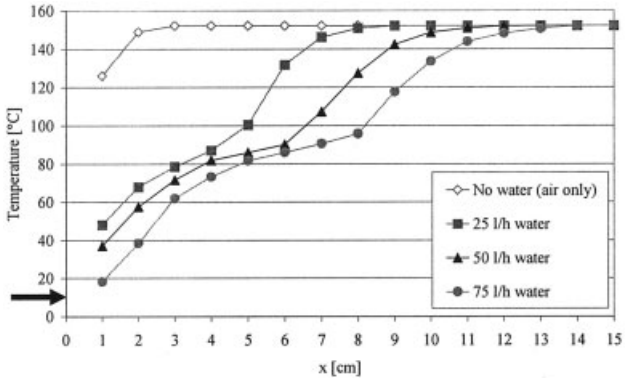

Figure 9. Mean temperatures along the distance *x* from the nozzle at *z* = 110 cm and *y* = 0 cm.

Internally mixed two-fluid fan nozzle no. 4, spray angle 60°. The liquid momentum fluxes are 0.031, 0.125, and 0.282 N; 8.3 m^3/h atomizing air; FCC bed at 153°C.

momentum of the atomizing gas dissipates not only in the process of liquid injection but also in transporting fluidized bed particles. Because the fraction of fluidized bed solids remains constant, more momentum dissipates in the process of liquid injection. On the other hand, the premixing of liquid feed and atomizing gas seems to provide momentum for a more effective injection and transport of fluidized bed solids.

It should be noted that the temperature profiles of internally and externally mixed two-fluid nozzles differ for the injection of air only, although the same volumetric fluxes of air have been used. The explanation is simply the difference in the spray pattern. The internally mixed nozzle has a fan spray of 60°, whereas the externally mixed nozzle has a full-cone spray of 20° spraying angle only, which results in a deeper penetration of the jet.

Such differences between externally mixed and internally mixed two-fluid nozzles are not known for the atomization in a gaseous environment.[18] From these results of the present experimental investigation, it can thus be deduced that the fluidized bed solids have a significant impact on the process of

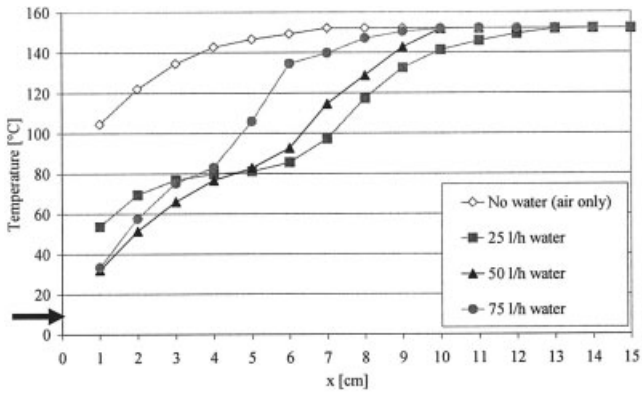

Figure 10. Mean temperatures along the distance *x* from the nozzle at *z* = 110 cm and *y* = 0 cm.

Externally mixed two-fluid full cone nozzle no. 3, spray angle 20°. The liquid momentum fluxes are 0.01, 0.039, and 0.088 N; 8.3 m^3/h atomizing air; FCC bed at 153°C.

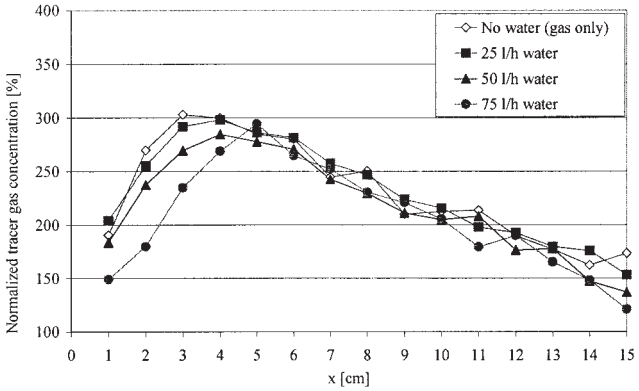

Figure 11. Local time-averaged tracer gas concentration along the distance *x* from the nozzle at *y* = 0 cm and *z* = 115 cm.

Internally mixed two-fluid fan nozzle no. 4, spray angle 60°. The liquid momentum fluxes are 0.031, 0.125, and 0.282 N; 8.3 m^3/h atomizing gas; FCC bed at 153°C.

atomization. The fluidized bed solids seem to hinder the process of atomization, if not to inhibit the generation of droplets.

Further evidence was given by an experimental investigation on the fate of the atomizing gas. The atomizing gas supplies the momentum not only for the dispersion of the liquid feed but also for the penetration into the fluidized bed. Copan et al.[22] found that the injection with a two-fluid nozzle performs in a manner similar to the penetration of gas jets into fluidized beds. This would imply that almost no momentum is needed for the dispersion of the liquid feed, which needs to be investigated for higher liquid loading. The above experiments on the liquid injection with internally mixed and externally mixed two-fluid nozzles were repeated in such a way that CO_2 tracer was mixed in the atomizing gas. The concentration of tracer gas near the nozzle exit was measured with suction probes. It was found that an "equilibrium concentration" is adjusted with sufficient distance from the nozzle exit. This equilibrium concentration is caused by the equilibrium of adsorption and desorption of CO_2 on the surface of FCC catalyst particles. The equilibrium concentration corresponds to the volume concentration, which is adjusted when the tracer gas is perfectly mixed with the fluidizing air. Therefore, the measured local gas concentrations were normalized by the equilibrium concentration. The tracer gas concentration was measured 5 cm above the spray axis. It should be noted that the tracer gas concentration was measured on a dry basis. The vaporized water was removed from the gas sample before the gas analysis, and is thus independent of the liquid feed rate. The results of these measurements are shown in Figures 11 and 12.

For the internally mixed two-fluid nozzle (Figure 10), the tracer gas concentration increases from 150 to 200% of the equilibrium concentration at $x = 1$ cm, reaches its maximum of 300% at $x = 4$–5 cm, and decreases with further distance from the nozzle exit until the equilibrium concentration is reached. Almost no difference can be found in the tracer profile for the injection of the gas jet only (no liquid) and the injection of 75 L/h of the test liquid. Given the measured changes in the corresponding temperature profile, the atomizing gas of internally mixed two-fluid nozzles seems to occupy a constant region only.

Different results were obtained for the injection with the externally mixed two-fluid nozzle (Figure 12). The profile for the injection of gas only is similar to the profile described above. Then, the maximum of the tracer gas concentration shifts toward the nozzle exit with increasing flow rate of the injected test liquid water. So the penetration depth of the atomizing gas into the fluidized becomes hindered with increasing liquid loading. This is in accordance with the finding that the penetration depth of the liquid feed is also decreasing with increasing liquid loading, as seen in the corresponding temperature profiles (cf. Figure 10).

The discussion of the measured profiles of the temperature and of the tracer gas concentration gives first indications of the mechanism of the liquid injection into fluidized beds. However, a major factor in this process is the distribution of the vaporized liquid feed.

A series of experiments was performed on the measurement of the vapor concentration in the fluidized bed. One of the key experiments was on the injection of the test liquid water with a fan nozzle having a spraying angle of 120°, where the temperature distribution is discussed in the context of Figure 7. There the nozzle's spray pattern was recognizable in the measured temperature distribution. The corresponding distribution of measured vapor concentrations is shown in Figure 13. Amazingly, to some extent the spray pattern (fan nozzle 120°) is also recognizable in the distribution of the vapor concentrations, given that it is in the distribution of mean temperatures in the fluidized bed. The measured vapor concentration reaches almost 100% for the first few centimeters near the nozzle exit. All vapor concentrations $> 50\%$ are marked by the color black in the chart. The vapor concentration decreases with further distance from the nozzle exit and asymptotically reaches an equilibrium concentration of 14.6 vol %. The adjustment of an equilibrium concentration is similar to the finding for the injection of the adsorptive tracer gas CO_2, which is caused by the equilibrium of desorption (drying) and adsorption of water on the surface of the porous catalyst particles. The equilibrium concentration of 14.6% corresponds to the volume concentration, which is adjusted when the vaporized liquid feed is perfectly mixed with the fluidizing air.

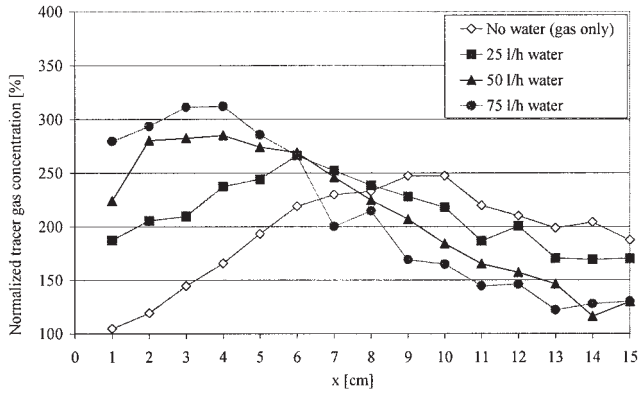

Figure 12. Local time-averaged tracer gas concentration along the horizontal distance *x* from the nozzle at *y* = 0 cm and *z* = 115 cm.

Externally mixed two-fluid full cone nozzle no. 3, spray angle 20°. The liquid momentum fluxes are 0.01, 0.039, and 0.088 N; 8.3 m^3/h atomizing gas; FCC bed at 153°C.

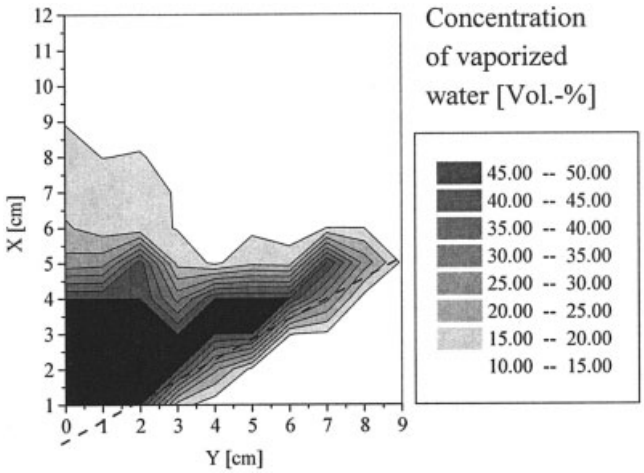

Figure 13. Time-averaged vapor concentration near the nozzle at z = 110 cm.

Single-fluid fan nozzle no. 2, spray angle 120°; 50 L/h water. The liquid momentum flux is 0.206 N; FCC bed at 153°C.

For a more detailed analysis, the vapor concentration was measured not only along the spray axis but also 5 cm above and 5 cm below. The results are shown in Figure 14, where the local vapor concentrations are normalized by the equilibrium concentration. The concentrations on the spray axis exhibit high values near the nozzle exit. These high vapor concentrations seem to be caused by liquids that stick and evaporate at the tip of the suction probes. It is striking that the vapor concentrations 5 cm above and below the spray axis are almost similar. If an instantaneous evaporation would occur at the nozzle exit, one would have found a significantly higher vapor concentration downstream (that is, at the measurement position 5 cm above the spray axis). Because the vaporizing feed is homogeneously distributed both up- and downstream, a transport of liquid droplets with the up-flowing gas phase seems to be unlikely. Such a homogenous distribution may be caused by the erratic motion of the fluidized bed solids, which are wetted at the nozzle exit and transported into the interior of the

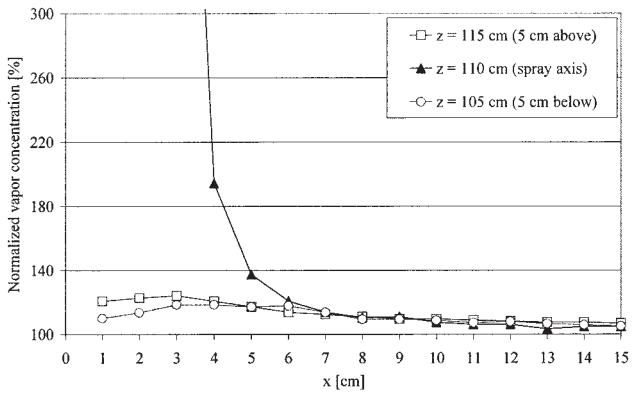

Figure 14. Time-averaged vapor concentration along the distance x from the nozzle at y = 0 cm.

Single-fluid fan nozzle no. 2, spray angle 120°; 50 L/h water. The liquid momentum flux is 0.206 N; FCC bed at 153°C.

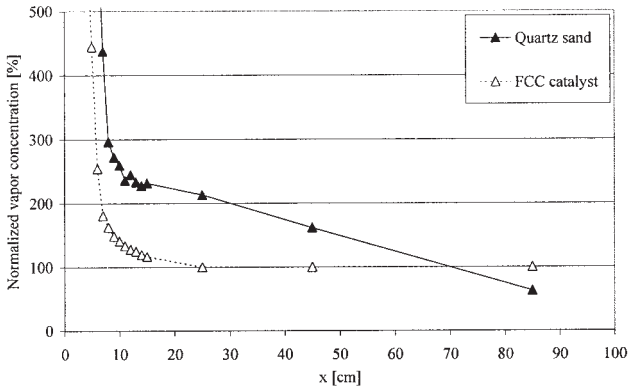

Figure 15. Time-averaged vapor concentrations along the x-axis at y = 0 cm and z = 115 cm.

Two-fluid full-cone nozzle no. 3, spray angle 20°; 50 L/h water. The liquid momentum flux is 0.039 N; 8.3 m^3/h atomizing air, bed at 153°C.

fluidized bed, where the liquid then evaporates from the particles' surfaces.

This finding of wetted particles is in keeping with the already discussed idea that the fluidized-bed solids hinder the atomization of liquid feed. In the case of porous catalyst particles, the liquid feed may be taken up into the pores and the release of vapor is slowed down by the moderate drying rates of porous material. The adsorption of vapor at the surface of dry particles is also an important factor.

However, the dominance of adsorption effects is unlikely in high-temperature applications such as BASF's aniline process[3] or the phthalic anhydride synthesis.[25] To model this situation, another set of experiments was performed with quartz sand as the fluidized bed material. Quartz sand is nonporous; thus neither is liquid taken up into the pores nor is vaporized feed adsorbed. A comparison was made between the profile of vapor concentration, which was measured in a fluidized bed of quartz sand, and of FCC catalyst. The local vapor concentration was normalized by the equilibrium concentration and the results are shown in Figure 15. The measured vapor concentration in a bed of FCC catalyst decreases steeply with increasing distance from the nozzle exit and asymptotically reaches the equilibrium concentration at x = 25 cm. The profile in a bed of quartz sand does not have such a characteristic. It was observed for quartz sand that the measured vapor concentrations exhibit numerical values above the equilibrium concentration over a distance of up to 70 cm from the nozzle exit. The vapor concentration decreases with further distance from the nozzle exit and concentrations were measured below the equilibrium concentration.

It is unlikely that enhanced evaporation occurs for the nonporous fluidized-bed material of quartz sand. One possible explanation may be that agglomerates are formed near the nozzle exit, thus capturing the injected liquid. These agglomerates are more stable and stick to the tip of the suction probes over a wider distance from the nozzle exit. Agglomerates of porous FCC catalyst are obviously less stable because the captured liquid is taken up and the agglomerates break up more easily. However, these effects are difficult to conclude from the results of vapor concentration and temperature measurements only.

Therefore, the capacitance measurement technique was used for the detection of liquids that move either freely or in ag-

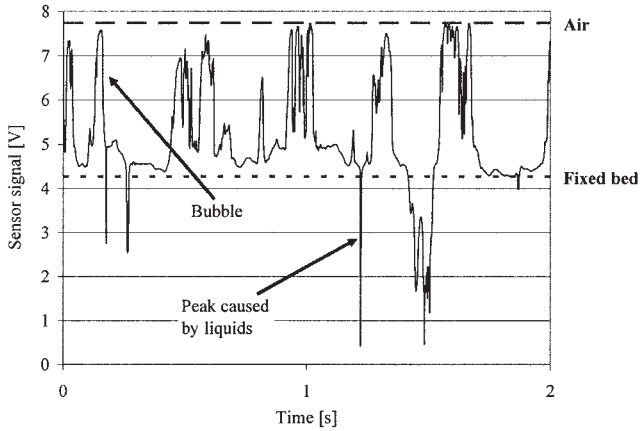

Figure 16. Sequence of capacitance measurement signals at $x = 7$ cm, $y = 0$ cm, and $z = 110$ cm.

Two-fluid full-cone nozzle no. 3, spray angle 20°; 50 L/h water. The liquid momentum flux is 0.039 N; 8.3 m^3/h atomizing air; FCC bed at 153°C.

glomerates. Because the dielectric constant of liquid water is extremely high compared to the dielectric constants of gas and solids, respectively, liquid water will cause clear signals of the capacitance measurement system. Additionally, the measurement system with needle capacitance probes assists not only in the local detection of the test liquid water but also in the determination of the local solids volume concentration.

A typical time series is shown in Figure 16 that was measured at a distance of $x = 7$ cm from the nozzle exit. The signal level with the characteristic value of 7.74 V for air is depicted in the chart as a dashed line. The signal level with the characteristic value of 4.27 V for the fixed bed of FCC catalyst particles is depicted in the chart as a dotted line. The signal levels of air and of a fixed bed of solids, respectively, were obtained from external calibration of the capacitance probe.

The flow structure of a fully developed bubbling fluidized bed can be identified in the given time series. Bubbles are characterized by a peak from the signal baseline of gas–solid suspension up to the signal level of air, as marked in the chart. Bubbles can be identified at a typical mean frequency of bubbling fluidized beds at 2–3 Hz.[25] Because this bubbling frequency was measured in a fluidized bed with and without liquid injection, it was concluded that the gas–solid flow structure is almost unaffected by the liquid injection. Occasionally, peaks were monitored during the measurement with a higher capacitance than that of the fixed bed of solids. These peaks are attributed to the presence of liquids. It was found that liquids were detected in the suspension phase only, thus providing further evidence for the idea that these signals were caused by wetted particles and/or agglomerates. The frequency of agglomerates in these time series was higher in fluidized beds of quartz sand than that in FCC catalyst.

The direct portability of the above experimental results to technical applications of the liquid injection into fluidized bed reactors is limited because of the test liquid water. Water exhibits an extremely high heat of evaporation of 2500 kJ/kg, which differs significantly from that of heats of evaporation of liquids in technical applications. Thus, additional experiments were performed with the test liquid ethanol. Ethanol is an organic substance and has a lower heat of evaporation of 730 kJ/kg. With such a low heat of evaporation and a boiling point of 78°C at ambient pressure, ethanol is also highly volatile at mean fluidized bed temperatures of 150°C.

The test liquid ethanol was injected into the fluidized bed by use of the externally mixed two-fluid nozzle of full-cone spray pattern. The fluidized bed material was FCC catalyst in one set of experiments and quartz sand in another set of experiments. The fluidized bed was operated at a superficial gas velocity of 0.3 m/s and the mean temperature was kept constant at 153°C.

The results of the temperature measurements are shown in Figure 17. To assess the performance of the test liquid water, temperature profiles of the respective experiments with water are also shown in the graph. It can be seen that the temperature profiles of both test liquids exhibit a similar characteristic. Evidently, no instantaneous evaporation occurs at the nozzle exit not even for the highly volatile test liquid ethanol. The temperature rises steeply from the inlet temperature of 20°C to a characteristic temperature at 10 K below the boiling point (that is, about 90°C for water and 70°C for ethanol). This characteristic temperature is another indication for the formation of agglomerates at the nozzle exit. If there were droplets or individual particles with wetted surfaces, the temperature would be either the wet bulb temperature for excess air or the boiling temperature for limited mass transfer of vapor. The reduction in temperature accounts for agglomerates.

It might be argued that the difference in the vapor densities between water and ethanol, respectively, might explain the difference in the penetration depth. However, because no instantaneous evaporation of the liquids was observed, but rather a moderate drying process of wetted solids, the differences in the vapor densities should not have a significant effect on the local temperature and the gas–solid flow in the fluidized bed.

With further distance from the nozzle exit, the temperature increases to the mean temperature of the fluidized bed. The agglomerates decay in this region and become mixed into the interior of the fluidized bed by the large-scale mixing of the solids. In general, the temperature profile reaches deeper into the fluidized bed for the injection into a fluidized bed of quartz sand than into a fluidized bed of FCC catalyst. The agglomer-

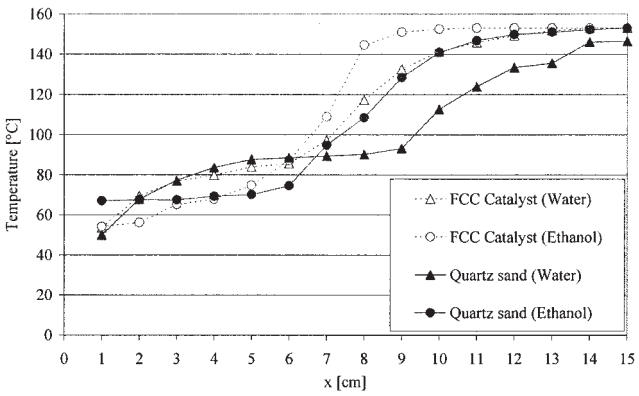

Figure 17. Local time-averaged temperatures along the distance x from the nozzle at $z = 110$ cm and $y = 0$ cm.

Two-fluid full-cone nozzle no. 3, spray angle 20°; 25 L/h ethanol or water. The liquid momentum fluxes are 0.0078 and 0.010 N; 8.3 m^3/h air; fluidized bed at 153°C.

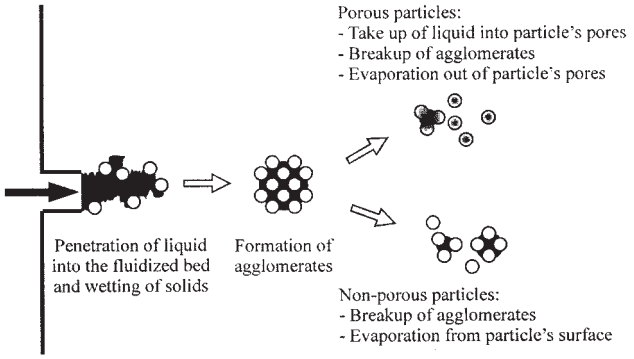

Figure 18. Mechanism of the liquid injection into a dense (bubbling) fluidized bed.

ates of quartz sand particles are obviously more stable than agglomerates of FCC catalyst. This was also observed in the profiles of vaporized feed, as discussed in the context of Figure 15. Another factor is the take-up of liquids into pores and the resulting slower drying rate of porous FCC catalyst.

Conclusions

Based on the results of the present experimental investigation, a new model is suggested for the mechanism of the injection of liquid reactants into fluidized bed reactors, which is illustrated by Figure 18. The liquids are locally introduced into the fluidized bed reactor with the aid of an injector nozzle. Despite the fact that the reactor is operated at temperatures well above the boiling point of the injected liquid, no instantaneous evaporation occurs at the nozzle exit. Instead, the liquid jet penetrates the fluidized bed and wets the fluidized bed solids in the vicinity of the nozzle exit. The presence of solids at a high solids volume concentration of 30–40% seems to suppress the atomization of the injected liquids. Because the injected liquids and the solids come into direct contact at the nozzle exit, it seems that—contrary to what is known from the atomization in a gaseous environment—no liquid droplets are formed within the dense bubbling fluidized bed (cf. Figure 1).

Particles become transported into the liquid jet and immediately form agglomerates after all. These agglomerates become rapidly transported into the interior by the gross solids mixing of the fluidized bed. The liquid evaporates from the interior of the agglomerates. The agglomerates decay because of the impact of the vigorous particle–particle interactions in the fluidized bed. In the case of porous particles, the liquid is also taken up into the inner pores. Therefore, agglomerates of porous particles break up more easily but the drying rate is slowed down because of the pore diffusion. If the vapor adsorbs at the particles' surface, a more homogeneous pattern of released vapor can be observed to arise from the equilibrium of desorption (drying) and adsorption.

Based on these findings a model for the scale-up of fluidized bed reactors with liquid injection has been developed,[23,24] a model that assumes the instantaneous wetting of the fluidized bed particles at the nozzle exit and considers the transport of the wetted particles by the gross solids mixing of the fluidized bed. The release of the vaporized feed should be modeled by experimentally determined drying kinetics, which account not only for the properties of the injected liquid but also for the properties of the fluidized bed particles.

Acknowledgments

The authors gratefully acknowledge the financial support of this research project by the Deutsche Forschungsgemeinschaft, Bonn.

Literature Cited

1. Werther J. Fluidized-bed reactors. *Ullmann's Encyclopedia of Industrial Chemistry*. Weinheim, Germany: Wiley–VCH; 2001.
2. Wilson JW. *Fluid Catalytic Cracking Technology and Operations*. Tulsa, OK: PennWell Publishing, 1997.
3. Kahl T, Schroeder KW, Lawrence FR, Marshall WJ, Hoeke H, Jaehk R. Aniline. *Ullmann's Encyclopedia of Industrial Chemistry*. Weinheim, Germany: Wiley–VCH; 2001.
4. Burdett ID, Eisinger RS, Cai P, Lee KH. Gas-phase fluidization technology for production of polyolefins. In: Yang WC, Li J, Kwauk M, eds. *Fluidization X*. New York, NY: United Engineering Foundation; 2001:39-52.
5. Theologos KN, Markatos NC. Advanced modeling of fluid catalytic cracking riser-type reactors. *AIChE J.* 1993;39:1007-1017.
6. Theologos KN, Lygeros AI, Markatos NC. Feedstock atomization effects on FCC riser reactors selectivity. *Chem. Eng. Sci.* 1999;54: 5617-5625.
7. Gao J, Xu C, Lin S, Yang G. Simulations of gas–liquid–solid 3-phase flow and reaction in FCC riser reactors. *AIChE J.* 2001;47:677-692.
8. Gupta A, Rao DS. Effect of feed atomization on FCC performance: Simulation of entire unit. *Chem. Eng. Sci.* 2003;58:4567-4576.
9. Heinrich S, Mörl L. Fluidized bed spray granulation—A new model for the description of particle wetting and of temperature and concentration distribution. *Chem. Eng. Process.* 1999;38:635-663.
10. Becher RD, Schlünder EU. Fluidized bed granulation: Gas flow, particle motion and moisture distribution. *Chem. Eng. Process.* 1997; 36:261-269.
11. Smith PG, Nienow AW. On atomizing a liquid into a gas fluidized bed. *Chem. Eng. Sci.* 1982;37:954-956.
12. Maronga SJ, Wnukowski P. Establishing temperature and humidity profiles in fluidized bed particulate coating. *Powder Technol*. 1997; 94:181-185.
13. Fan LS, Lau R, Zhu C, Voung K, Warsito W, Wang X, Liu G. Evaporative liquid jets in gas–liquid–solid flow system. *Chem. Eng. Sci.* 2001;56:5871-5891.
14. Gu W, Tuzla K, Chen JC. Measurement of liquid spray evaporation in fast fluidized beds. *AIChE Symp. Ser.* 1996;92:153-154.
15. Skouby DC. Hydrodynamic studies in a 0.45-m riser with liquid feed injection. *AIChE Symp. Ser.* 1999;95:67-70.
16. Newton D, Fiorentino M, Smith GB. The application of X-ray imaging to the developments of fluidized bed processes. *Powder Technol.* 2001;120:70-75.
17. Knapper BA, Gray MR, Chan EW, Mikula R. Measurement of efficiency of distribution of liquid feed in a gas–solid fluidized bed reactor. *Int. J. Chem. Reactor Eng.* 2003;1:A35.
18. Lefebvre AH. *Atomization and Sprays*. London: Hemisphere; 1989.
19. Sirignano WA. *Fluid Dynamics and Transport of Droplets and Sprays*. Cambridge, UK: Cambridge Univ. Press; 1999.
20. Zhu C, Wang X, Fan LS. Effect of solids concentration on evaporative liquid jets in gas–solid flows. *Powder Technol.* 2000;111:79-82.
21. Wiesendorf V, Werther J. Capacitance probes for solids volume concentration and velocity measurements in industrial fluidized bed reactors. *Powder Technol.* 2001;119:143-157.
22. Copan J, Clarke N, Berruti F. The interaction of single- and two-phase jets and fluidized beds. In: Yang WC, Li J, Kwauk M, eds. *Fluidization X*. New York, NY: United Engineering Foundation; 2001:77-84.
23. Bruhns S. On the Mechanism of Liquid Injection into Fluidized Bed Reactors. PhD Dissertation, Technical University Hamburg–Harburg, Germany; 2002.
24. Bruhns S, Werther J. Modeling the injection of liquid reactants into fluidized bed reactors. *Proc. of 8th China–Japan Symposium, Fluidization 2003—Science and Technology*, Tokyo, Japan: Society of Chemical Engineers Japan, 2003:386-396.
25. Kunii D, Levenspiel O. *Fluidization Engineering*. Stoneham, MA: Butterworth-Heinemann; 1991.

Manuscript received Jan. 12, 2004, and revision received Jun. 28, 2004.